NJC

Accepted Manuscript

This is an *Accepted Manuscript*, which has been through the Royal Society of Chemistry peer review process and has been accepted for publication.

Accepted Manuscripts are published online shortly after acceptance, before technical editing, formatting and proof reading. Using this free service, authors can make their results available to the community, in citable form, before we publish the edited article. We will replace this *Accepted Manuscript* with the edited and formatted *Advance Article* as soon as it is available.

You can find more information about *Accepted Manuscripts* in the Information for Authors.

Please note that technical editing may introduce minor changes to the text and/or graphics, which may alter content. The journal's standard Terms & Conditions and the Ethical guidelines still apply. In no event shall the Royal Society of Chemistry be held responsible for any errors or omissions in this *Accepted Manuscript* or any consequences arising from the use of any information it contains.

ROYAL SOCIETY OF CHEMISTRY

www.rsc.org/njc

Table of Contents

Langmuir adsorption isotherm demonstrates monolayer drug loading with hyperhydrophilic three dimensional crosslinked polymers. Furthermore, pseudo order kinetics was also evaluated.

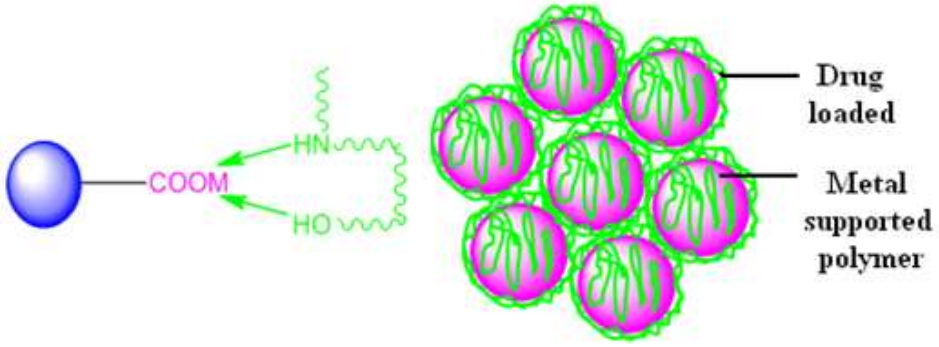

Hyperhydrophilic three dimensional crosslinked beads as effective drug carrier in acidic medium: adsorption isotherm and kinetics appraisal

Sachin Mane, Surendra Ponrathnam, Nayaku Chavan*

Polymer Science and Engineering Division

National Chemical Laboratory

Pune – 411008, India

Ph.: 91-20-25903008

E-mail: nn.chavan@ncl.res.in

ABSTRACT

Conventional drug delivery materials are known to provide slow and less drug loading in aqueous medium due to hydrophobic or less hydrophilic properties of the carrier. However present study was interested in synthesis of cheaply available metals modified hyperhydrophilic polymer. Hyperhydrophilic three dimensional crosslinked beads as a drug carrier was synthesized with desirable properties that substantially influence polymer efficiency. These synthesized polymers were characterized for surface area, particle size, acid content, morphology and metal modification was evaluated to obtain efficient polymer for drug adsorption in acidic medium. Contact time that significantly affect to drug adsorption was comparatively evaluated with respect to cheaply available cobalt and nickel metals. Interestingly adsorption study revealed that initial 12 h is the gradual drug loading afterwards adsorption increased steadily and goes towards stabilization. Furthermore, theoretical predictions of adsorption including Langmuir adsorption isotherm and pseudo order of kinetics were also evaluated. Remarkably, Co/Ni modified polymer demonstrated 85 and 78% metoprolol drug adsorption respectively at

optimum pH 3 and 24 h. Langmuir adsorption isotherm revealed monolayer adsorption with Co/Ni modified polymer. Pseudo first and second order kinetics was also evaluated demonstrated adsorption mechanism and equilibrium adsorption capacity respectively.

Keywords

Adsorption isotherm, Adsorption kinetics, Hyperhydrophilic, Metoprolol, Three dimensional crosslinking

Introduction

Over the past few years, drug loading using nanoparticles has been studied intensively.[1–6] Nanoparticle possesses high surface area, smaller particle size and agglomeration/aggregation characteristics.[7] Recently, there has been growing interest in nickel nanoparticles in organic synthesis,[8–11] due to their easy preparation, high catalytic activity, possible processibility, high stability and easy recyclability compared to normal Raney nickel. Yan et al. demonstrated[12] the high catalytic activity whereas Khurana et al. showed[13] the higher stability and efficiency of nickel nanoparticles. Nickel stabilized polymer have been used for coupling reaction, whereas cobalt stabilized polymer used for alkene epoxidation.[14, 15] Polymer based functional materials attract considerable attention in various fields due to their specific properties.[16–18] Nowadays researchers synthesized the various types of nanoparticles, for instance, Wilczewska et al. discussed[19] the nanoparticles based on liposomes, solid lipids, polymer, dendrimer, silica, carbon and magnetic nanoparticles having different properties. In 2011, Neamtu et al. studied[20] the applications of Co, Ni nanoparticles in magnetic resonance imaging and targeted drug release.

Metal supported polymers are of great interest and ubiquitous material due to their excellent chemical, physical and catalytic properties. Nowadays polymer application in different areas is an emerging field.[21–23] Recently Prijic et al. discussed[24] the biocompatibility and

biomedical applications of nanoparticles. In addition to biocompatibility, carrier properties are the major concern for high drug loading. Porous and crosslinked polymer is attracted to researchers due to its wide applicability in different fields such as biomedical and solid phase synthesis.[25] Extensive research is going on with metal stabilized polymer due to their biocompatibility, insoluble, porous and rigid property. Among the transition metals Cu, Co, Ni received considerable public interest due to their cheaply available, good optical, electrical, thermal and magnetic properties.[26–29]Aforementioned metals are cost effective compared to metals such as Ag, Au and Pt. Hence, they are potentially used in drug delivery and catalysis. Researchers published much more work on gold and silver metals rather than inexpensive cobalt, copper, nickel and iron metals. Increased attention has been achieved for transition metal supported polymer especially Ni, Co, Fe due to their inexpensive and electronegative properties.[30–32] It is worth noting that copolymer applications in drug adsorption is effective due to the properties of copolymer such as porosity, surface area, particle size and thermostability are highly tunable changing physico-chemical parameters such as stirring speed, porogen, crosslinker over other drug carrier materials.

Undertaken study is novel and has not been reported earlier. To the best of our knowledge hyperhydrophilic, three dimensionally crosslinked polymer beads with cobalt/nickel supported polymer for drug profile is not studied elsewhere. In present work, hyperhydrophilic three dimensionally crosslinked polymer was synthesized to obtain better efficiency in aqueous medium due to its hydrophilic properties. However, micron sized particle having high surface area, metal stabilized crosslinked polymer that attributes to awesome results[33, 34] was synthesized and its applications in drug adsorption has been studied. At most, nanoparticle may suffer through conglomeration that significantly affect drug loading. As result, present work is

interested to synthesize micron sized polymer and evaluating efficiency of metal supported polymer in drug loading. Moreover, higher drug adsorption was obtained with cobalt over nickel modified polymer. At most, Langmuir adsorption and pseudo order of kinetics rarely studied with respect to drug loading. Langmuir adsorption isotherm is in good agreement with parameter studied. This work promises to give excellent adsorption drug profile with comparative metal responsive study. One of the aims of this study is to develop hydrophilic, robust, cost effective, environmentally benign, recyclable metal supported polymer recognized as effective drug carrier. Furthermore, metal supported polymer can be useful in catalytic study in functional group transformation.[35–38] Drug used in adsorption study is represented below,

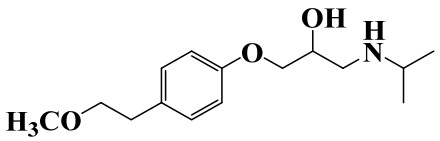

Metoprolol

Experimental

Materials

Acrylic acid (>99%) was procured from Merck (Mumbai), pentaerythritol tetraacrylate (>99%) was purchased from Sigma-Aldrich (USA), cobaltous chloride hexahydrate (99%) from Sdfine (Boisar), azobisisobutyronitrile (98%) from AVRA synthesis Pvt. Ltd (Hyderabad, India), poly(vinyl pyrrolidone) K90 powder (PVP, mol. wt.: 360,000) was procured from Fluka. Chlorobenzene (99.5%), nickel chloride hexahydrate (98%) and sodium borohydride (97%) were procured from Loba chemie (Mumbai). All chemicals were used as received.

Characterization

FTIR samples were prepared in KBr pellets after drying the copolymers at 80^{o}C for 8 h. FTIR spectra were recorded on Perkin Elmer spectrophotometer FTIR spectrometer (KBr) (Perkin Elmer, model: Spectrum GX; serial number: 69229, number of scans: 10 numbers, resolution: 4 cm^{-1}, interval: 1 cm^{-1}), Surface area of copolymers was evaluated by surface analyzer using (NOVA 2000e Quantachrome instruments, Boynton, FL-33426) by BET (nitrogen adsorption) method. Average particle diameter was determined using Accusizer 780 (model LE 2500-20) PSS.NICOMP Particle sizing system, Santa Barbara, California, USA. Acid content was determined by KOH using titrimetric method. Thermal stability (DTG) of copolymers was studied by simultaneous thermal analysis (STA, Perkin Elmer), while glass transition temperature was evaluated by differential scanning calorimetry Q10 (Thermal analysis). Scanning electron microscopy (SEM) was used for external morphology whereas particle visualization as well as EDX analysis performed by Quanta 200-3D, dual beam ESEM microscope, Netherland with thermionic emission tungsten filament as electron source.

Preparation of aqueous and organic phase

Aqueous phase (1 wt %) was prepared by dissolving the protective colloid (PVP) in deionised water. However organic phase prepared by mixing monomer (acrylic acid), crosslinker (pentaerythritol tetraacrylate), initiator (AIBN) and pore generating solvent (chlorobenzene) in nitrogen atmosphere at room temperature.

Synthesis of copolymers

Specially designed reactor having diameter 14 cm and height 20 cm was used to carry out suspension polymerization. Reactor was assembled with a constant temperature water bath,

mechanical stirrer, condenser and nitrogen gas inlet. Organic (discontinuous) phase containing monomer, crosslinker, initiator and porogen slowly added to the aqueous (continuous) phase under stirring at 500 rpm in nitrogen overlay. Later on, reaction temperature was raised to 70^{o}C and stirred for 3 h. Furthermore, spherical copolymer beads obtained were thoroughly washed with water, methanol and finally with acetone and dried at 60^{o}C under reduced pressure. However, synthesized copolymer beads were further purified with methanol in a soxhlet extractor and dried at 60^{o}C for 8 h under reduced pressure. As a consequence of three reactive double bonds, synthesized polymer forms three dimensional more stable polymer networks. Poly(AA-co-PETRA) was synthesized in presence of chlorobenzene named as APCH with CLD ranges from 5 to 25%.

Synthesis of metal supported polymer by aqueous reduction method

Poly(AA-co-PETRA) synthesized by suspension polymerization was modified with cobalt/nickel by well known aqueous reduction method. A 5 g of $CoCl_2 \cdot 6H_2O$ or $NiCl_2 \cdot 6H_2O$ was dissolved in 20 mL deionised water separately. Solution of $CoCl_2 \cdot 6H_2O$ or $NiCl_2 \cdot 6H_2O$ in deionised water (10 mL) was added to 10 g base polymer (APCH) of 5 and 25% CLD. This mixture was placed 30 h for uniform adsorption of cobalt/nickel salt. Polymer sample containing metal salt solution was dried at 80^{o}C for 5 h. Subsequently, sodium borohydride (1 g) aqueous solution in 5 mL deionised water used to reduce the dried metal salt supported polymer.[39, 40] Sodium borohydride aqueous solution was added dropwise to the polymer-cobalt chloride or polymer-nickel chloride mixture at room temperature till effervescences stops completely. In order to avoid the metal oxidation, reaction was carried out in nitrogen atmosphere. This mixture was placed under stirring for 5 h. Subsequently, polymer mixture was filtered and washed with deionised water till neutral pH of filtrate. Later on, polymer was dried at 70^{o}C for 5 h under

reduced pressure. This dried sample was used for characterization. Overall, copolymer was synthesized by suspension polymerization, subsequently modified with two metals separately by aqueous reduction method. Hydrophilic poly(AA-co-PETRA) synthesis and Co/Ni metal supported polymer is represented in Schemes 1 and 2 respectively.

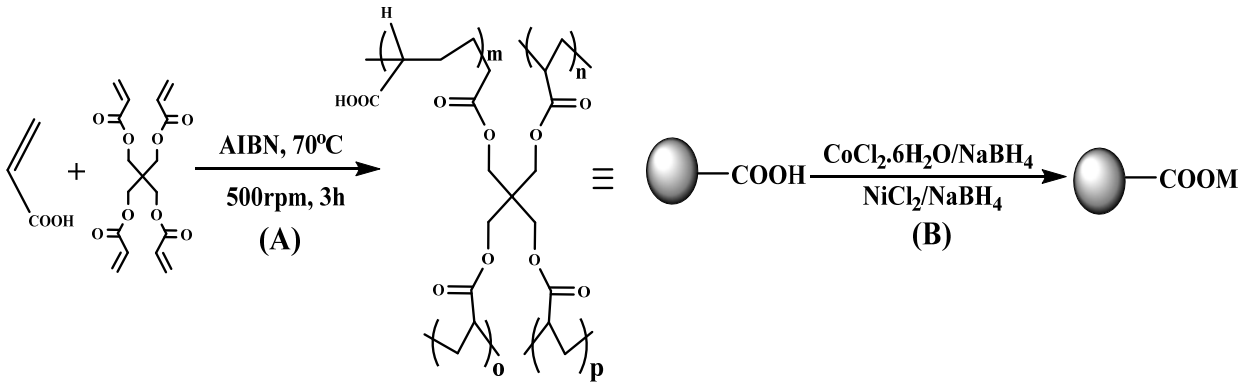

Acrylic acid | Pentaerythritol tetraacrylate | Three dimensionally crosslinked poly(AA-co-PETRA) | Co/Ni modified poly(AA-co-PETRA)

M = Co/Ni

Scheme 1 Synthesis of poly(AA-co-PETRA) by suspension polymerization and Co/Ni modified poly(AA-co-PETRA).

Comparative drug loading evaluation

Drug loading with respect to two different metals was evaluated separately with UV spectroscopy. A 20 mg Co/Ni MSP added to 30 mL capacity glass vial containing 20 mL (25 ppm) drug solution prepared in buffer solutions having pH 3 at room temperature. In order to attain accomplished contact between metal and drug in buffer solution, sample vials were placed under shaking at room temperature. Sample was removed after certain interval of time to analyze UV absorbance. Subsequently, equilibrium drug adsorption study was carried out at room temperature using 20 mL (50 ppm) solution with both metals and pH 3 buffer solution. Experimental procedure and conditions were same as aforementioned in contact time study.

Sample was removed at 24 h to analyze drug absorbance. Drug adsorption reaction scheme is represented in Scheme 2.

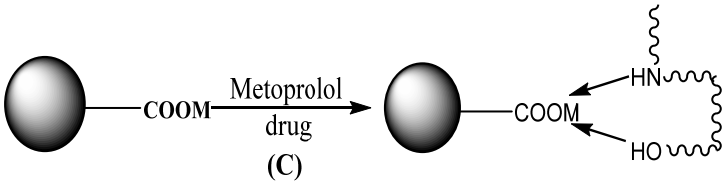

Co/Ni modified three dimensional polymer Metoprolol loaded Co/Ni modified polymer

Scheme 2 Co-ordinate complex formation between Co/Ni MSP and metoprolol drug.

Results and discussion

Monomer-crosslinker feed composition

[Two sentences deleted] In present work hyperhydrophilic poly(AA-co-PETRA) was synthesized using chlorobenzene as pore generating solvent by suspension polymerization at 5, 10, 15, 20 and 25% CLD in the form of beads. Crosslink density defines the percent moles of crosslinking agent (PETRA) relative to moles of acrylic acid monomer. Feed composition of monomer, crosslinker and reaction conditions used in suspension polymerization is reported in Table 1.

Table 1 Feed composition of poly(AA-co-PETRA).

Monomer system	Units	Crosslink density (%)				
		5	10	15	20	25
Acrylic acid: Pentaerythritol tetraacrylate	mol	0.192: 0.010	0.163: 0.016	0.141: 0.021	0.125: 0.025	0.112: 0.028
	g	13.797: 3.373	11.721: 5.731	10.188: 7.472	9.010: 8.81	8.075: 9.87

Reaction conditions: Batch size = 16 mL, AIBN = 2.5 mol%, stirring speed = 500 rpm, reaction time = 3 h, outer phase = H_2O, protective colloid = poly(vinylpyrrolidone), concentration of protective colloid = 1%, porogen = chlorobenzene, porogen concentration = 48 mL (monomer: porogen ratio, 1:3 v/v).

Fourier transform infrared (FTIR) spectroscopy

FTIR spectroscopy (KBr) was used to confirm the synthesis of base and metal modified polymer. Base polymer poly(AA-co-PETRA) illustrated presence of broad hydroxyl peak corresponds to 3447 cm^{-1} and 2986 cm^{-1} corresponds to –C–H str. whereas peak at 2500 cm^{-1} assigned to hydrogen bonded O–H str. (broad). Acid functionality assigned to 1719 cm^{-1}. Furthermore, peak at 1471 cm^{-1} attributes to C–H deformation (in-plane). Moreover, 1409 cm^{-1} relates to symm. –COO– str. and ester functionality of PETRA gets overlap with –COOH functionality of acrylic acid whereas 1188 and 959 cm^{-1} assigned to –C–OH vib. The peak at 985 cm^{-1} corresponds to C–H deformation (out-of plane). Cobalt modified polymer demonstrated that the acid peak converted into ester and shifted towards 1738 cm^{-1}. However, –COO– symm. str. corresponding to 1407 cm^{-1}. Similarly, nickel modified polymer indicated acid peak shifting[41] towards 1739 cm^{-1}. Moreover, 1418 cm^{-1} corresponds to –COO– symm. str. It is worth noting that there is small peak in the range of 3400–3500 cm^{-1} with revealed attenuation in absorbance and augmentation in transmittance strongly support to presence of small acid functionality. This is mainly due to acid groups are well buried into polymer matrix are not available for modification and are easily available for FTIR evaluation. FTIR spectra of base and modified polymer were illustrated in Fig. 1.

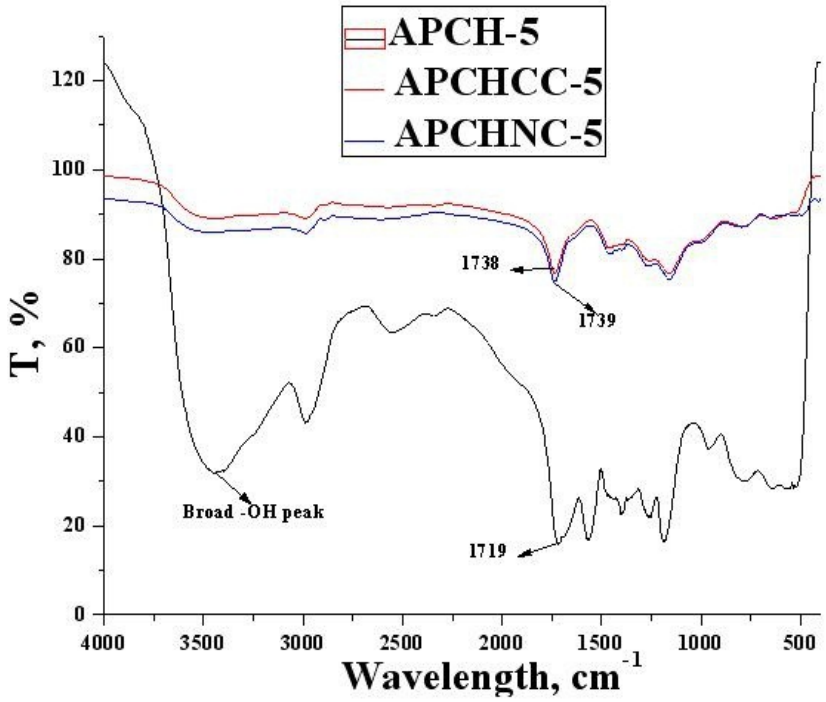

Fig. 1 FTIR spectrum of base (APCH-5) and MSP (APCHCC-5 and APCHNC-5).

Surface area determination

Polymer surface area substantially influences the polymer efficiency. As result, surface area of synthesized poly(AA-co-PETRA) and modified polymer (MSP) evaluated at 5 and 25% CLD. It seems that base polymer has surface area 60.90 and 78.57 m^2/g at 5 and 25% CLD respectively. In addition, cobalt and nickel MSP revealed surface area 52.49 and 29.47 m^2/g at 5% CLD respectively. It appears that surface area augmented with higher CLD.[42, 43] On the other hand, surface area of Co/Ni MSP slightly attenuated compared to base polymer due to metal binding at 5% CLD. Thus to balance higher surface area and more reactivity of base polymer, APCH polymer at 5% CLD selected for drug adsorption profiling.

Particle size distribution

Researchers published much more work on nanoparticles synthesis and its applications in drug loading.[44, 45] However; present work was focused on the synthesis of micron sized particles

for drug loading application perspectives. Owing to average particle size in the range of 15–30 μm, MSP can be easily separated and recovered by filtration because particle sizes above 1 μm difficult pass through filter unlike nanoparticles. In still another aspect micron sized particles able to improve metal (Co/Ni) modification due to their non-conglomerated characteristics resulting fast drug adsorption. Besides, nanoparticle has aggregation properties that influence drug adsorption. One of the aims of present work is to investigate effect of micron sized particles for adsorption drug profile. Average particle size of base and Co/Ni MSP was determined for CLD 5 to 25%. Results elucidate that particle size of base polymer attenuated with higher CLD perhaps due to higher CLD increases concentration of crosslinker[46] resulting strong binding between monomer and crosslinker allowed to attenuate particle size. However, Co/Ni MSP display little increase in particle size compared with base polymer. This is due to surface modification of base polymer with metal. Average particle size, before and after modification of polymer is demonstrated in Fig. 2A whereas particle size distribution is represented in Fig. 2B.

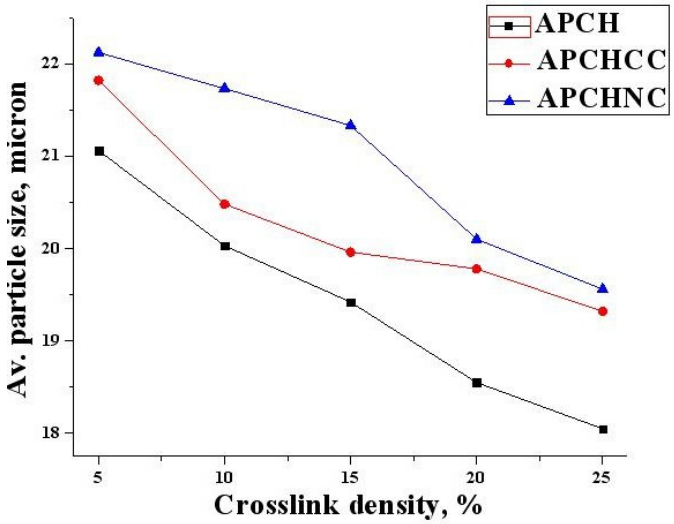

Fig. 2A Average particle size of base (APCH-5) and MSP (APCHCC-5 and APCHNC-5).

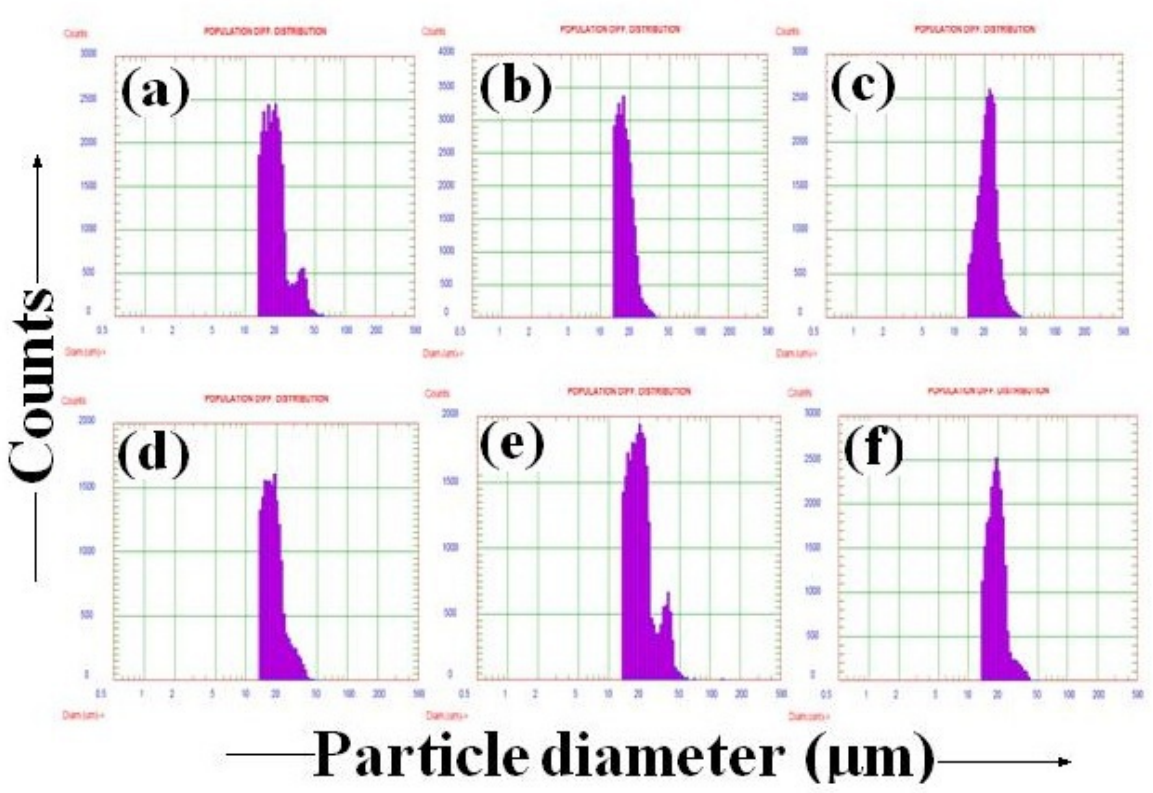

Fig. 2B Particle sized distribution of (a) APCH-5 (b) APCH-25 (c) APCHCC-5 (d) APCHCC-25 (e) APCHNC-5 (f) APCHNC-25.

Acid content determination

Indeed, polymer efficiency depends on many factors such as surface area, porosity, non-conglomerated property, particle size and so on. On the other hand, polymer reactivity depends on the functional group content available in the polymer matrix. In present work, carboxylic acid based and three dimensionally crosslinked poly(AA-co-PETRA) was synthesized and its acid content was evaluated. In order to estimate the polymer reactivity, acid content of synthesized base polymers were determined titrimetrically from 5 to 25% CLD by well known KOH method.[47] Dried base polymers were used for acid content determination. Theoretical acid content were 11.24, 9.44, 8.144, 7.15 and 6.4 mmol/g whereas observed result demonstrated

3.35, 2.52, 2.00, 1.61 and 1.37 mmol/g of acid content at 5, 10, 15, 20 and 25% CLD. Result clearly illustrated that observed acid content is much lower than theoretical due to large number of acid functionality is well buried into polymer matrix consequently not available for titrimetric determination. Furthermore, experimental acid content attenuated with higher CLD. This is mainly due to acrylic acid concentration substantially attenuated with higher CLD. However, available acid content at 5% CLD is sufficient for metal modification. Theoretical and observed acid content is demonstrated in Fig. 3.

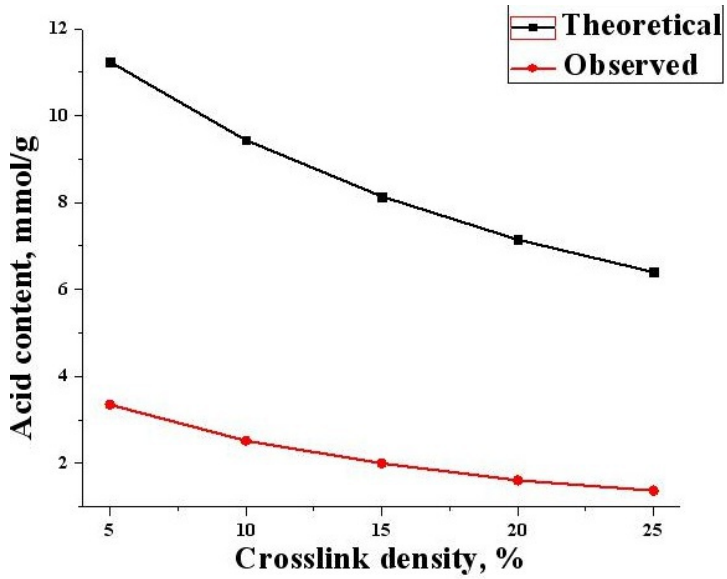

Fig. 3 Theoretical and observed acid content (mmol/g) of base polymer (APCH) at different crosslink density.

Thermogravimetric analysis (DTG)

Due to vast applications of MSP not only at room temperature but at high temperature also, its thermostability study became essential.[48] A number of research papers published around the world to develop recoverable catalysts with desirable properties. In present investigation, MSP having high surface area and extremely hydrophilic characteristics were synthesized to use

in aqueous as well as alcoholic solvents. Thermogravimetric analysis of copolymer at different CLD performed by simultaneous thermal analysis (Perkin Elmer) from 50–800^{o}C under nitrogen atmosphere with heating rate 10^{o}C/min. Differential thermogravimetric (DTG) analysis of base polymer (APCH) at 5 and 25% CLD was evaluated. In addition, DTG of cobalt and nickel MSP at 5 and 25% CLD was also studied. DTG thermogram elucidated that, Tmax of base polymer (APCH) is 458 and 447^{o}C at 5 and 25% CLD respectively. Moreover, Co MSP displays 422 and 392^{o}C whereas Ni MSP displays 402 and 383^{o}C at 5 and 25% CLD respectively. Crosslinker has flexible property consequently allowed attenuating Tmax. Thus, owing to more concentration of flexible crosslinker[43] at 25% CLD in base as well as MSP both attenuated in Tmax at 25% compared to 5% CLD. In still another aspect, cobalt modified polymer attenuated maximum decomposition temperature (Tmax) whereas nickel modified polymer revealed further attenuation in Tmax. DTG results are illustrated in Fig. 4.

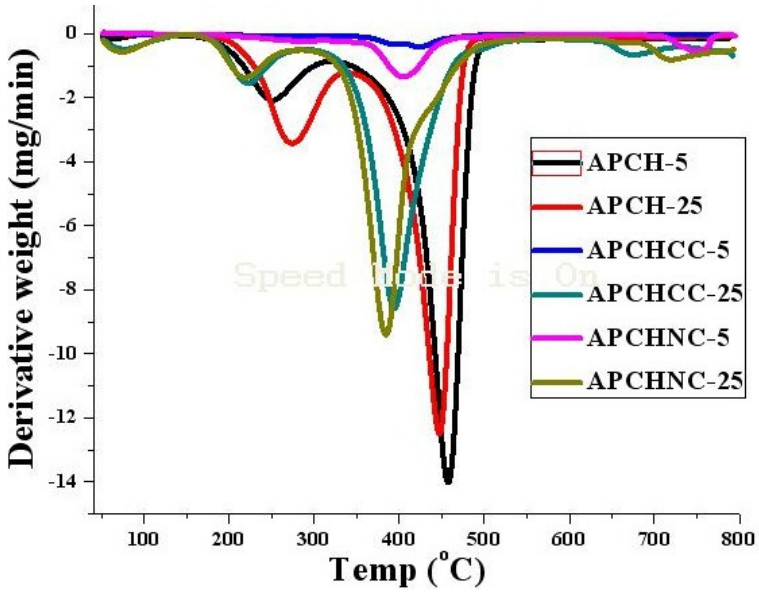

Fig. 4 DTG thermogram of base (APCH-5, 25) and MSP (APCHCC-5, 25 and APCHNC-5, 25).

Differential scanning calorimetry (DSC) analysis

Recent years, there has been tremendous research has been performed in solid state chemistry because of industrially economical and environmentally benign of recyclable polymer support. Nowadays applications of polymers are growing interest in organic synthesis at room[49] as well as high temperatures.[50] Properties of polymer support are highly tunable changing physical and chemical reaction parameters according to the requirements. MSP should be used at or below glass transition temperature (Tg). MSP used at or above Tg attributes to physical as well as chemical interaction between MSP and reactants or products. Thus Tg helps to decide safe temperature of MSP in organic reactions. Similarly, industrial application of Co/Ni MSP as catalysis provides much more efficacy due to their recover, recycle, reuse and inexpensiveness. DSC study implies that glass transition temperature (Tg) of base polymer (APCH) is 235 and 220^{o}C at 5 and 25% CLD respectively. Moreover, cobalt MSP (APCHCC) display 225 and 200^{o}C whereas nickel MSP (APCHNC) display 233 and 206^{o}C at 5 and 25% CLD respectively. The trend of Tg observation is same like DTG consequently reason of difference in Tg of base and Co/Ni MSP with respect to CLD is same as aforementioned in thermogravimetric study. Figure 5 demonstrated the Tg of base and metal modified polymer.

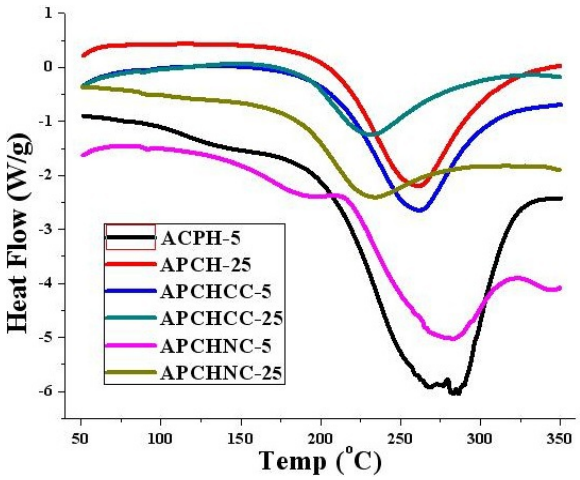

Fig. 5 DSC thermogram of base (APCH-5, 25) and MSP (APCHCC-5, 25 and APCHNC-5, 25).

External morphology study

Scanning electron microscope (SEM) image is the visual observation pictorial tool. SEM images of base and Co/Ni MSP were scanned with 500x magnification at 5 and 25% CLD. However, SEM display external morphology as well as particle size distribution of polymers obtained by suspension polymerization. Base polymer implies spherical, non-conglomerated and rigid morphology. Moreover, metal binding surface morphology of Co/Ni polymer also scanned by SEM. It is auspicious that polymer beads are spherical and non conglomeration in nature even after modification of polymers. SEM images of base and metal modified is illustrated in Fig. 6.

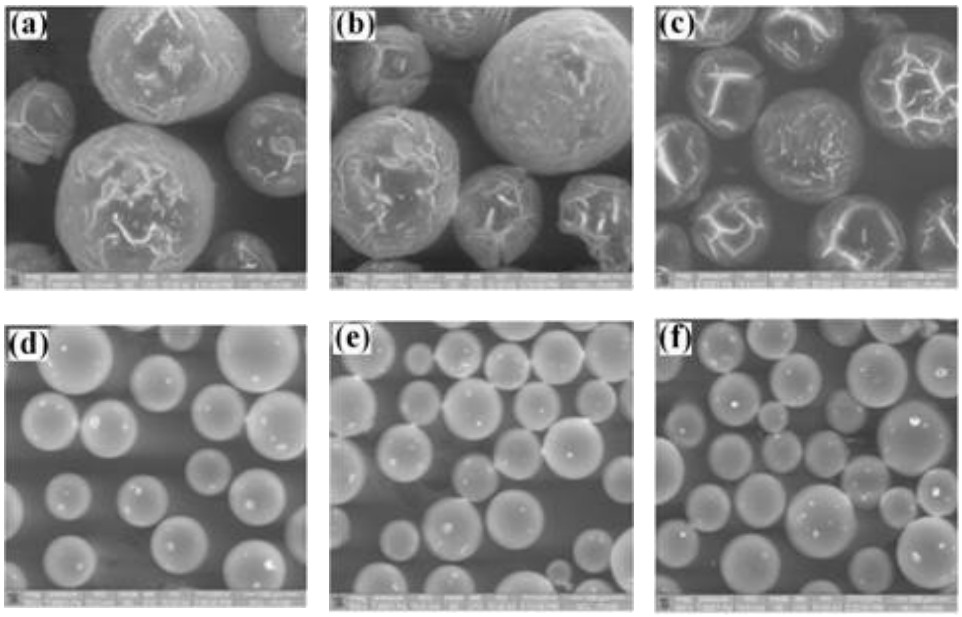

Fig. 6 Scanning electron microscopy images of APCH, APCHCC, and APCHNC at 5% (a, b, c) and 25% (d, e, f) crosslink density respectively at 500x magnification.

Qualitative and quantitative metal determination

Energy dispersive X-ray (EDX) is one of the most important tools for qualitative and quantitative metal determination. In present work, EDX analysis of base polymer (APCH) and Co/Ni MSP was evaluated at 5 and 25% CLD. It implies that base polymer contain carbon and

oxygen only. On the other hand cobalt MSP contains 14.4, 5.1 wt% cobalt whereas nickel MSP contain 10.8, 7.4 wt% nickel at 5 and 25% crosslink density respectively along with carbon and oxygen in different concentrations. Unfortunately hydrogen can not determine due to instrument limitation. Since, more reactive sites (acid content) available at lower CLD, higher percentage of metal Co/Ni was obtained at low CLD (5%) polymer, inversely less percentage of metal Co/Ni was observed at higher CLD (25%) polymer. Perhaps, this is due reactivity difference of polymer at different CLD. Owing to high surface are, acid functionality possibly may modify outer as well as internal surface with Co or Ni metal.

Drug loading study by spectrometric method

Recently different techniques are available to evaluate drug adsorption profile. Most widely used method is UV spectrometric method. In present work drug loading was studied by UV spectrometric method analyzing drug absorbance. Metoprolol drug solution standardization was carried out by absorbance measurement of different drug concentration (5, 10, 15, 20 and 25 ppm) in deionised water at wavelength 220 nm. Highest correlation coefficient was in better agreement (R^2 = 0.999). Effect of contact time on metal responsive drug loading was investigated.

Effect of contact time on adsorption rate

In 2014, Aleanizy et al. carried out the adsorption capacity of Metronidazole[51] with the use of kaolin from the pH 1.2 to 8.0. They demonstrated that adsorption goes on increasing with increase in pH. However, they showed that 10 mg Metronidazole adsorbed per gram of kaolin at pH 1.2. In present study synthesized polymers are hyperhydrophilic and stable towards acids and alkali due to three dimensionally crosslinked network.[52]As a consequence, polymer beads work very well in acidic medium. Effect of contact time is crucial parameter that attributes to drug

adsorption. Metoprolol drug loading with respect to cobalt/nickel was studied at different time intervals. Metoprolol absorbance implies that initial 12 h is the exponential exalted period for drug with Co/Ni MSP. After 12 h, gradual loading was observed with Co/Ni MSP. Furthermore, Co MSP is more effective rather than Ni MSP due to more surface area and modification of Co MSP rather than Ni MSP. At 24 h, metoprolol adsorption was 85 and 78% with Co/Ni MSP at 5% CLD respectively. Besides, after 24 h metoprolol adsorption gets stabilized due to drug saturation with metal reactive sites in MSP. Effect of contact time on adsorption is illustrated in Fig. 7.

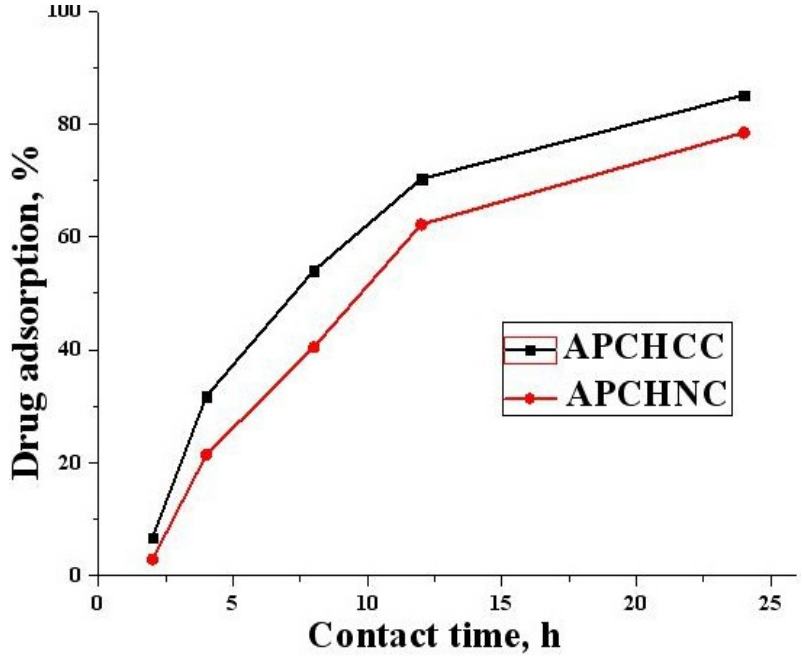

Fig. 7 Effect of contact time on metoprolol loading.

In still another aspect, equilibrium adsorption was carried out to confirm maximum adsorption of drug that helps to study the Langmuir adsorption isotherm. It is important to notice that metoprolol adsorption observed was 13.5 and 15 mg/g of Co/Ni MSP at 5% CLD respectively.

Langmuir adsorption isotherms

Adsorption isotherm is the theoretical prediction of drug adsorption i.e. to confirm either mono or bilayer adsorption. Langmuir adsorption isotherm was carried out at room temperature for metoprolol drug with comparative investigation of cobalt and nickel adsorption rate at pH 3. Adsorption study was fitted by least square method to linearly transformed Langmuir adsorption isotherm. Linear Langmuir adsorption isotherm[53, 54] represented by Eq. (1):

$$\frac{Ce}{qe} = -\frac{1}{Qob} + \frac{Ce}{Qo} \quad (1)$$

where, Ce is the equilibrium conc. (mg/L), qe (mg/g) is the amount of drug adsorbed per gram at equilibrium, Q_0 (mg/L) and b are the Langmuir constants related with drug adsorption capacity and adsorption energy respectively.

Results obtained by adsorption study conducted at room temperature were fitted with linear Langmuir adsorption isotherm Eq. (1). Highest correlation coefficient (R^2) for Co MSP (R^2=1) and Ni MSP (R^2=1) are in good agreement with parameter studied. Results confirm that the adsorption was monolayer due to better agreement of highest correlation coefficient. Langmuir adsorption isotherm of metoprolol with respect to cobalt and nickel is shown in Fig. 8.

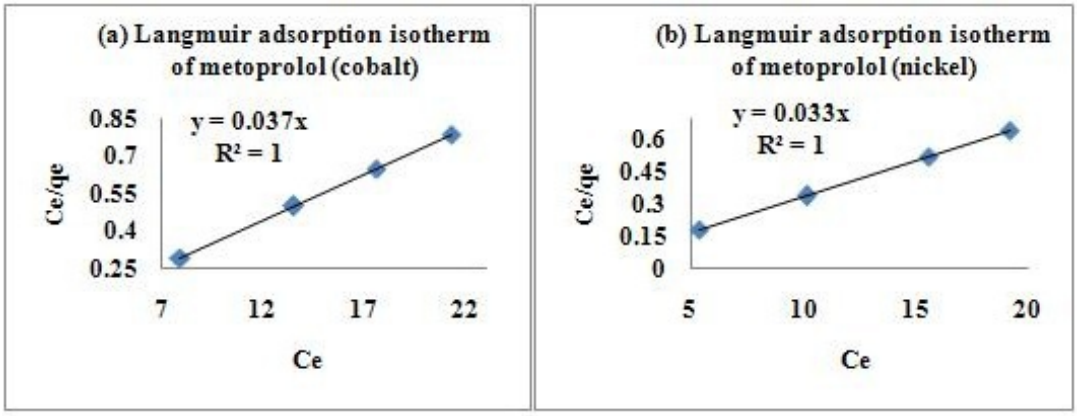

Fig. 8 Langmuir adsorption isotherm of metoprolol with (a) Co MSP and (b) Ni MSP.

Pseudo first order kinetics

Kinetic models are not only applicable to estimate sorption rates but also reaction mechanism. In this study, pseudo first and second order kinetic models were investigated. Subsequently, two different isotherms were applied to present study to investigate the sorption dynamics of metoprolol with respect to cobalt and nickel MSP. Kinetic and equilibrium adsorption are two important physicochemical parameters considered during sorption dynamics study. Kinetic adsorption describes the relationship between contact time and drug adsorption rate whereas equilibrium adsorption describes the distribution of drug between solid-liquid phases and determining the feasibility and capacity of the drug for adsorption. Nowadays number of models is available to explain the mechanism of drug adsorption. More preferably used kinetic model is pseudo first order Lagergren kinetic[55, 56] Eq. (2):

$$\log(q_e - q_t) = \log q_e - \frac{K_{ad}t}{2.303} \quad (2)$$

where, qe is the mass of drug adsorbed at equilibrium (mg/g), qt (mg/g) is the mass of drug adsorbed at time t, and Kad is the first order kinetics constant (L/min).

Pseudo first order determines the rate of occupation of adsorption sites is proportional to the number of unoccupied sites. Plot of log(qe-qt) versus t revealed a straight line demonstrated the application of the first order kinetic model. Pseudo first order kinetics of metoprolol adsorption is illustrated in Fig. 9.

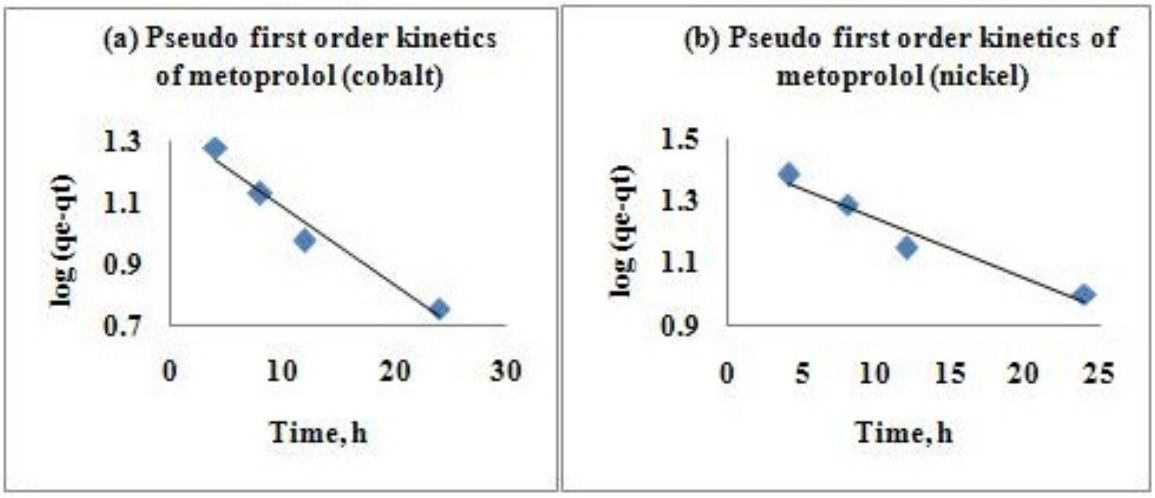

Fig. 9 Pseudo first order kinetics of metoprolol with (a) Co MSP and (b) Ni MSP.

Pseudo second order kinetics

Pseudo second order kinetic equation was applied to the present study to determine the equilibrium capacity of cobalt/nickel MSP and demonstrated[55, 57] by Eq. (3):

$$\frac{t}{q_t} = \frac{1}{K_{2ad} q_e^2} + \frac{t}{q_e} \quad (3)$$

where, K_{2ad} is the second order kinetics rate equilibrium constant (g/ mg·min), q_e is the equilibrium adsorption of drug, q_t is the adsorption of drug at time t.

Second order kinetic model display linear relationship with respect to adsorption capacity (Fig. 10). In this model physicochemical interaction between Co/Ni polymer supported metal and drug solution in aqueous medium attributes for drug removal. Plot of t/qt versus t was plotted for equilibrium adsorption capacity study. Equilibrium adsorption of metoprolol carried out at room temperature indicated linear increases in adsorption of drugs with respect to time using Co/Ni MSP. Pseudo second order kinetics of metoprolol adsorption is illustrated in Fig. 10.

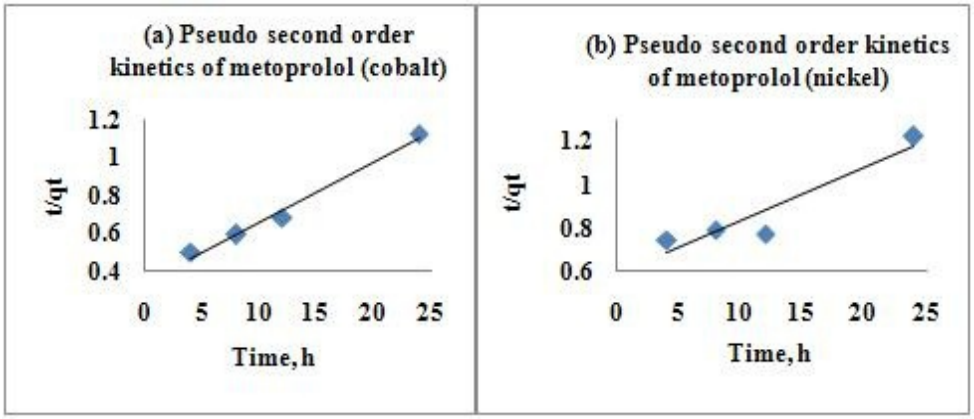

Fig. 10 Pseudo second order kinetics of metoprolol with (a) Co MSP and (b) Ni MSP.

Conclusions

In conclusion, hyperhydrophilic and three dimensional crosslinked polymer beads was synthesized and successfully modified with Co/Ni metals separately. It is worth noting that cobalt metal supported polymer revealed higher adsorption rather than nickel metal supported polymer. However, contact time study demonstrated that 85 and 78% metoprolol loading was observed with respect to Co and Ni respectively at pH 3 and 24 h. Both metal supported polymers imply gradual exalt in adsorption of metoprolol till 12 h, subsequently adsorption is stabilized due to saturation of reactive sites. In the drug loading aspect, surface area of carrier is the most important attributing parameter followed by metal electronegativity. Langmuir adsorption isotherm was well fitted with parameter studied and demonstrated adsorption is monolayer. Pseudo first and second order kinetics illustrated drug removal mechanism and adsorption capacity respectively. Thus high surface area, more reactive, micron sized and three dimensionally crosslinked polymer beads became successful in drug loading study. Owing to insoluble property of polymer, metal supported polymer can be recover, recycle and reuse in different applications which make them industrially economical, environmentally benign.

Acknowledgment

This research was financially supported by University Grant Commission (UGC), New Delhi, India. We express our gratitude towards UGC for the award of research fellowship (Fellowship Award No.: 20/06-2010 (IEU–IV).

Abbreviations

APCH-5: Acrylic acid–pentaerythritol tetraacrylate–chlorobenzene at 5% CLD.

APCHCC-5: Acrylic acid–pentaerythritol tetraacrylate–chlorobenzene–cobalt chloride at 5% crosslink density.

APCHNC-5: Acrylic acid–pentaerythritol tetraacrylate–chlorobenzene–nickel chloride at 5% CLD.

MSP: Metal supported polymer.

CLD: Crosslink density.

References

1 K. S. Soppimath, T. M. Aminabhavi, A. R. Kulkarni and W. E. Rudzinski, *J. Controlled Release*, 2001, **70,** 1–20.

2 I. I. Slowing, B. G. Trewyn, S. Giri and V. S. Y. Lin, *Adv. Funct. Mater.*, 2007, **17,** 1225–1236.

3 W. H. De Jong and P. J. Borm, *Int. J. Nanomed.*, 2008, **3(2),** 133–149.

4 R. Ravichandran, *Int. J. Green Nanotechnol.: Biomed.*, 2009, **1,** B108–130.

5 R. Ma and L. Shi, *Polym. Chem.*, 2014, **5**, 1503–1518.

6 M. Hofmann-Amtenbrink, B. V. Rechenberg and H. Hofmann, *Nanostruct. Mater. Biomed. Appl.,* 2009, 119–149.

7 H. Golmojdeh and M. A. Zanjanchi, *Cryst. Res. Technol.,* 2012, **47(9),** 1014–1025.

8 P. Saha, M. A. Ali and T. Punniyamurthy, *Org. Synth.,* 2011, **88,** 398–405.

9 H. J. Xu, Y. F. Liang, Z. Y. Cai, H. X. Qi, C. Y. Yang and Y. S. Feng, *J. Org. Chem.,* 2011, **76,** 2296–2300.

10 J. F. Sonnenberg, N. Coombs, P. A. Dube and R. H. Morris, *J. Am. Chem. Soc.,* 2012, **134,** 5893–2899.

11 T. Ramani, P. Umadevi, K. L. Prasanth and B. Sreedhar, *Eur. J. Org. Chem.,* 2013, 6021–6026. DOI: 10.1002/ejoc.201300909.

12 J. M. Yan, X. B. Zhang, S. Han, H. Shioyama and Q. Xu, *Inorg. Chem.,* 2009, **48,** 7389–7393.

13 J. M. Khurana and K. Vij, *J. Chem. Sci.,* 2012, **124(4),** 907–912.

14 P. Styring, C. Grindon and C. M. Fisher, *Catal. Lett.,* 2001, **77(4),** 219–225.

15 G. Kowalski, J. Pielichowski and M. Jasieniak, *Appl. Catal. A,* 2003, **247,** 295–302.

16 H. Xiao, J. F. Stefanick, X. Jia, X. Jing, T. Kiziltepe, Y. Zhang and B. Bilgicer, *Chem. Commun.,* 2013, **49**, 4809–4811.

17 C. N. Kotanen, A. N. Wilson, C. Dong, C. Z. Dinu, G. A. Justin and G. E. Anthony, *Biomater.,* 2013, **34,** 6318–6327.

18 G. E. Anthony, C. Dong and C. Z. Dinu, *J. Mater. Chem.,* 2012, **22,** 19529–19539.

19 A. K. Salunkhe, R. J. Dias, K. K. Mali, N. S. Mahajan and V. S. Ghorpade, *Der Pharmacia Lettre,* 2011, **3(3),** 147–160.

20 J. Neamtu and N. Verga, *Digest J. Nanomater. Biostruct.,* 2011, **6(3),** 969–978.

21 B. R. Schroeder, M. I. Ghare, C. Bhattacharya, R. Paul, Z. Yu, P. A. Zaleski, T. C.

Bozeman, M. J. Rishel and S. M. Hecht, *J. Am. Chem. Soc.*, 2014, **136,** 13641–13656.

22 Z. Yu, R. M. Schmaltz, T. C. Bozeman, R. Paul, M. J. Rishel, K. S. Tsosie and S. M. Hecht, *J. Am. Chem. Soc.*, 2013, **135,** 2883−2886.

23 C. Bhattacharya, Z. Yu, M. J. Rishel and S. M. Hecht, *Biochem.*, 2014, **53,** 3264−3266.

24 S. Prijic and G. Sersa, *Radiol. Oncol.*, 2011, **45(1),** 1–16.

25 L. Ren, C. Teng, L. Zhu, J. He, Y. Wang, X. Zuo, M. Hong, Y. Wang, B. Jiang and J. Zhao, *Nanoscale Res. Lett.*, 2014, **9,** 163.

26 K Luyts, D Napierska, B Nemery and P. H. M. Hoet, *Environ. Sci.: Processes Impacts,* 2013, **15,** 23.

27 U. Saxena and P. Goswami, *J. Nanopart. Res.*, 2012, **14,** 813–823.

28 N. Jha and S. Ramaprabhum, *J. Phys. Chem. C,* 2008, **112,** 9315–9319.

29 K. O. Santos, W. C. Elias, A. M. Signori, F. C. Giacomelli, H. Yang and J. B. Domingos, *J. Phys. Chem. C,* 2012, **116,** 4594–4604.

30 C. Nwosu, *J. Tech. Sci. Technol.*, 2012, **1(2),** 25–28.

31 L. Luo and S. Li, *J. Nat. Gas Chem.*, 2004, **13,** 45–48.

32 Y. J. Cho, D.C. Lee, H. J. Lee, K. C. Kim and Y. C. Park, *Bull. Korean Chem. Soc.*, 1997, **18(3),** 334–336.

33 N. K. Lunev, V. L. Struzhko and Y. I. Shmyrko, *Theor. Exp. Chem.*, 2002, **38(5),** 308–312.

34 Y. Rong, R. M. Evans, M. Carta, N. B. McKeown, G. A. Attard and F. Marken, *Electroanal.*, 2014, **26,** 904–909.

35 B. C. Ranu, K. Chattopadhyay, L. Adak, A. Saha, S. Bhadra, R. Dey and D. Saha, *Pure Appl. Chem.*, 2009, **81(12),** 2337–2354.

36 A. N. Vasiliev, E. A. Gulliver, J. G. Khinast and R. E. Rimana, *Surf. Coat. Technol.,*

2009, **203,** 2841–2844.

37 R. J. Kalbasi and N. Mosaddegh, Bull. *Korean Chem. Soc.,* 2011, **32(8),** 2584–2592.

38 K. Babak, B. Hesam, F. Elham, J. Ehsan and Z. Asghar, *Curr. Org. Synth.,* 2010, **7(6),** 543–567.

39 Z. Ghoranneviss, S. W. Gosavi and M. Limayee, *Iran. Phys. J.,* 2007, **1(2),** 25–30.

40 J. M. Khurana and K. Vij, *J. Chem. Sci.,* 2012, **124(4),** 907–912.

41 W. X. Tu, *Chin. J. Polym. Sci.,* 2008, **26(1),** 23–29.

42 A. Kotha, C. R. Rajan, S. Ponrathnam, K. K. Kumar and J. G. Shewale, *Appl. Biochem. Biotechnol.,* 1998, **74,** 191–203.

43 S. Mane, S. Ponrathnam and N. Chavan, *Eur. Polym. J.,* 2014, **59,** 46–58.

44 K. Cho, X. Wang, S. Nie, Z. Chen and D. M. Shin, *Clin. Cancer Res.,* 2008, **14,** 1310–1316.

45 I. I. Slowing, B. G. Trewyn, S. Giri and V. S. Y. Lin, *Adv. Funct. Mater.,* 2007, **17,** 1225–1236.

46 S. Banerjee, G. Chaurasia, D. Pal, A. K. Ghosh, A. Ghosh and S. Kaity, *J. Sci. Ind. Res.,* 2010, **69,** 777–784.

47 A. I. Vogel, Elementary Practical Organic Chemistry Part-III, Quantitative Organic Analysis, (Lond.), 1958, **Chapter XVI,** 667–671.

48 J. Pielichowski, G. Kowalski and G. Zaikov, *Chem. Chem. Technol.,* 2011, **5(3),** 303–308.

49 A. Shaabani, S. Keshipour, M. Hamidzad and M. Seyyedhamzeh, *J. Chem. Sci.,* 2014, **126(1),** 111–115.

50 G. Kowalski, J. Pielichowski and M. Grzesik, *Hindawi Pub. Corp. Sci. World J.,* 2014, **648949,** 1–9.

51 F. S. Aleanizy, F. Alqahtani, O. A. Gohary, E. E. Tahir and R. A. Shalabi, *Saudi Pharm. J.* 2014. DOI: 10.1016/j.jsps.2014.06.006.

52 V. P. Saxena, A Complete Course in ISC Chemistry, 2009, 9th edition, Vol. II, Chapter 22, 13.

53 H. Zheng, D. Liu, Y. Zheng, S. Liang and Z. Liu, *J. Hazard. Mater.,* 2009, **167,** 141–147.

54 M. B. Desta, *J. Thermodyn.,* 2013, **375830,** 1–6.

55 D. Robati, *J. Nanostruct. Chem.,* 2013, **3(55),** 1–6.

56 Y. S. Ho, *Scientometrics,* 2004, **59(1),** 171–177.

57 Y. S. Ho and G. McKay, *Process Biochem.,* 1999, **34,** 451–465.

Captions

Sr. no.	Description
Schemes	
1	Synthesis of poly(AA-co-PETRA) by suspension polymerization and Co/Ni modified poly(AA-co-PETRA).
2	Coordinate complex formation between Co/Ni MSP and metoprolol drug.
Tables	
1	Feed composition of poly(AA-co-PETRA).
Figures	
1	FTIR spectrum of base (APCH-5) and MSP (APCHCC-5 and APCHNC-5).

2 (A) Average particle size of base (APCH-5) and MSP (APCHCC-5 and APCHNC-5).

(B) Particle sized distribution of (a) APCH-5(b) APCH-25 (c) APCHCC-5 (d) APCHCC-25 (e) APCHNC-5 (f) APCHNC-25.

3 Theoretical and observed acid content (mmol/g) of base polymer (APCH) at different crosslink density.

4 DTG thermogram of base (APCH-5, 25) and MSP (APCHCC-5, 25 and APCHNC-5, 25).

5 DSC thermogram of base (APCH-5, 25) and MSP (APCHCC-5, 25 and APCHNC-5, 25).

6 Scanning electron microscopy images of APCH, APCHCC, and APCHNC at 5% (a, b, c) and 25% (d, e, f) crosslink density respectively at 500x magnification.

7 Effect of contact time on metoprolol loading.

8 Langmuir adsorption isotherm of metoprolol with (a) Co MSP and (b) Ni MSP.

9 Pseudo first order kinetics of metoprolol with (a) Co MSP and (b) Ni MSP.

10 Pseudo second order kinetics of metoprolol with (a) Co MSP and (b) Ni MSP.